Acta Crystallographica Section B
Structural Science
ISSN 0108-7681

Direct observation of arylnitrene formation in the photoreaction of arylazide crystals

Terufumi Takayama,[a] Takahiro Mitsumori,[a] Masaki Kawano,[a]‡ Akiko Sekine,[a]* Hidehiro Uekusa,[a] Yuji Ohashi[a]§ and Tadashi Sugawara[b]

[a]Department of Chemistry and Materials Science, Tokyo Institute of Technology, O-okayama, Meguro-ku, Tokyo 152-8551, Japan, and [b]Department of Basic Science, University of Tokyo, Komaba, Meguro-ku, Tokyo 153-8902, Japan

‡ Current address: Pohang University of Science and Technology, Hyoja-dong, Namgu, Pohang 790-784, Korea.
§ Ibaraki Quantum Beam Research Center, Shirakata, Tokai, Ibaraki 319-1106, Japan.

Correspondence e-mail: asekine@chem.titech.ac.jp

Received 17 March 2010
Accepted 13 September 2010

Seven crystal structures of arylazides, 2-azidobiphenyl (2), 4-(4-azidophenyl)butanoic acid (3), 3-azidobenzoic acid (4), *N*-(4-azidophenyl)acetamide (5), 2,4,6-trichlorophenyl azide (6), 2,5-dibromophenyl azide (7) and 2,4,6-tribromophenyl azide (8), have been analyzed by X-rays. When the crystals were irradiated with UV light at $\simeq 80$ K, only 2-azidobiphenyl gradually changed its cell dimensions with the retention of the single-crystal form. The crystal structure after photo-irradiation was analyzed by X-rays under the same conditions as those before photo-irradiation. Approximately 20% of the 2-azidobiphenyl molecule was converted to the triplet 2-biphenylnitrene and dinitrogen molecules. The existence of the triplet nitrene was confirmed by ESR and IR measurements. Although the structure of dinitrogen was clearly determined, the nitrene structure was obscure because the nitrene produced was almost superimposed on the original 2-azidobiphenyl. The other six crystals were non-reactive or easily broken when they were exposed to UV light. The different reactivity between 2-azidobiphenyl and the other compounds was successfully explained by the reaction cavity of the azido group.

1. Introduction

A reaction intermediate consisting of a phenyl group and an electrically neutral nitreno group, phenylnitrene, was proposed by Bertho when phenylazide was dimerized thermally, as shown in Scheme (I) (Bertho, 1924). The existence of the triplet phenylnitrene was confirmed as a reaction intermediate by ESR measurement (Smolinski *et al.*, 1962). The electronic spectra of phenylnitrene after photo-irradiation of phenylazide were reported in an organic matrix at 77 K (Reiser & Frazer, 1965; Reiser *et al.*, 1966). Since then, phenylnitrene and its derivatives, arylnitrenes, have created considerable interest owing to their potential applications to organic synthesis (Iddon *et al.*, 1979; Wentrup, 1981), photo-affinity labeling (Kotzyba-Hibert *et al.*, 1995) and materials science (Meijer *et al.*, 1988). Arylnitrenes are unstable substances and are difficult to trap because the nitreno group does not obey the octet rule. Several attempts have been made by organic and physical chemists to analyze reaction pathways involving an arylnitrene (Scriven, 1984; Platz, 1995; Borden *et al.*, 2000; Karney & Borden, 2001; Gritsan & Plats, 2001). Arylnitrenes revealed characteristic behaviors in the crystalline state which are different from those in solution, glass-matrices and gas states. It was reported that the half-lifetimes of arylnitrenes in the solid state were ~ 10 d at room temperature (Mahé *et al.*, 1992).

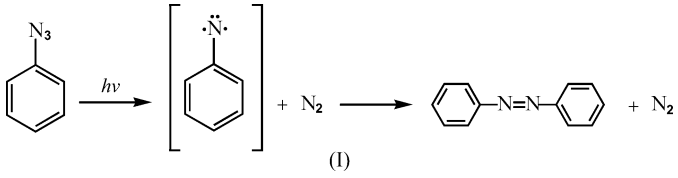

(I)

In a previous paper we reported the structures of 1-azido-2-nitrobenzene (1) before and after the photo-irradiation (Takayama *et al.*, 2003). It was clear that the reaction proceeded as shown in Scheme (II), since dinitrogen and benzofuroxan were observed in the crystal structure after photo-irradiation. However, it was impossible to observe the structure of the intermediate 2-nitrophenylnitrene, although a trace amount of the nitrene was observed in the IR spectra after photo-irradiation. In order to observe the structure of arylnitrene directly, several kinds of arylazide derivatives, as shown in Scheme (III), were prepared and the crystal structures before and after photo-irradiation were analyzed. The substituents of the arylazides were selected so as to expand the reaction cavity around the azido group. Crystals of the prepared arylazide derivatives, however, were non-reactive or easily broken on exposure to the UV lamp, except 2-azidobiphenyl (2). This paper shows the structure of the triplet 2-biphenylnitrene and the dinitrogen molecule after photo-irradiation and explains why the other arylazide crystals studied showed no reaction. Further X-ray studies to analyze the structures of the arylnitrenes have been performed using the technique of acid–base complex formation. The preliminary work has already been published (Kawano *et al.*, 2003) and further work is published in a separate paper (Mitsumori *et al.*, 2010).

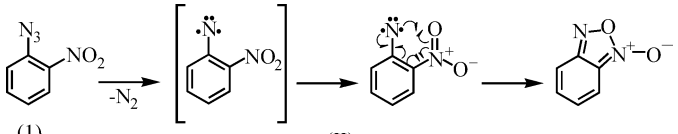

(1) (II)

2. Experimental

2.1. Preparation of arylazide derivatives

2.1.1. 2-Azidobiphenyl (2). 2-Aminobiphenyl (0.85 g, 5.0 mmol) and sodium nitrite (2.31 g, 33.5 mmol) were dissolved in a mixture of water (72 cm^3), diethyl ether (35 cm^3) and hydrochloric acid (30 cm^3) at 278 K. The solution was stirred for 2 h. Sodium azide (4.32 g, 66.5 mmol) in water (20 cm^3) was added at room temperature and stirred for 12 h. The organic layer was separated by a separating funnel and evaporated under reduced pressure until the oil was deposited. Desiccation of the oil under reduced pressure gave a brown solid as the crude product (0.58 g, 3.0 mmol, yield: 59%). Colorless crystals were obtained from toluene solution at 279 K. The other six compounds, (3), (4), (5), (6), (7) and (8), were prepared using similar methods, which are given in the supplementary material.[1]

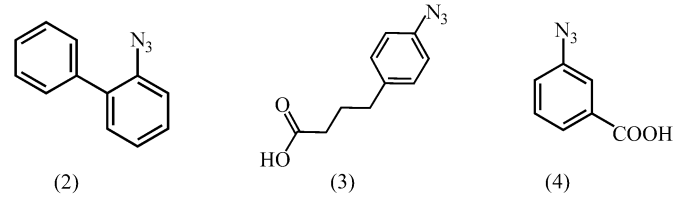

(2) (3) (4)

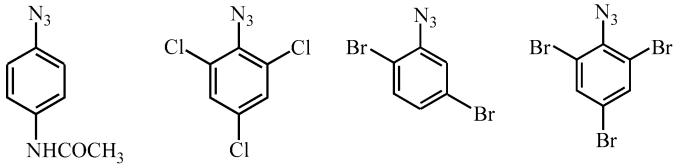

(5) (6) (7) (8)

(III)

2.2. IR spectra and theoretical calculation

2.2.1. FT-IR spectra. The FT-IR spectra were recorded in rapid scan mode with an Excalibur FTS 3000 instrument (Bio-Rad). A powdered sample of (2) dispersed in KBr pellets was attached to the cold finger of a He cryogenic refrigerator system (DAIKIN PS24SS). The sample was irradiated with a high-pressure Hg lamp (SAN-EI UVF-352S) with a band-path filter (Co-39 TOSHIBA, $\lambda = 390 \pm 50$ nm) through the double KBr windows of a temperature-controlled cell at 80 K for 2 h.

2.2.2. Theoretical calculation. Using the *GAUSSIAN*98 program, the optimized geometry of the triplet 2-biphenylnitrene was calculated at the (U)B3LYP/6-31G* level. The calculated vibrational frequencies obtained at the (U)B3LYP level were scaled by a factor of 0.97.

2.3. Single-crystal X-ray diffraction analysis

2.3.1. Data collection and reduction. Graphite-monochromated Mo $K\alpha$ radiation ($\lambda = 0.71073$ Å) was used with a Rigaku rotating anode X-ray generator and the temperature was controlled by the Rigaku cryostat system at ~ 80 K. All the diffraction data, except those for (4), were collected using a Bruker SMART-CCD diffractometer with four sets of ω-scan data (-32 to 146.2, 0.3° per frame) with $\chi = 54.83°$, $\varphi = 0$, 90, 180 and 270° for each set. These frame data were integrated using the *SAINT* (Bruker, 2007) program package. An empirical absorption correction was calculated with *SADABS* (Bruker, 2004*a*) and the space group was determined using *XPREP* (Bruker, 2004*b*). For (4) the diffraction data were collected on a Rigaku R-AXIS RAPID diffractometer on 44 oscillation photographs (each oscillation angle was 5° with no overlap margin) in the range $3.63 < \theta < 25.35°$. An empirical absorption correction was calculated using the *ABSCOR* program (Higashi, 1995) and the space group was determined with *TEXSAN* (Molecular Structure Corporation, 1999). The experimental details of seven crystals before irradiation are listed in Table 1.

[1] Supplementary data for this paper are available from the IUCr electronic archives (Reference: OG5042). Services for accessing these data are described at the back of the journal.

Table 1
Experimental details.

For (2) the corresponding data after photo-irradiation (2′) are given. Experiments were carried out with Mo $K\alpha$ radiation.

	(2)	(2′)	(3)	(4)
Crystal data				
Chemical formula	$C_{12}H_9N_3$	$C_{12}H_9N_3$	$C_{10}H_{11}N_3O_2$	$C_7H_5N_3O_2$
M_r	195.22	195.22	205.22	163.14
Crystal system, space group	Monoclinic, $P2_1/n$	Monoclinic, $P2_1/n$	Monoclinic, $P2_1/c$	Triclinic, $P\overline{1}$
Temperature (K)	83	83	80	80
a, b, c (Å)	5.6182 (2), 26.8034 (6), 6.9510 (2)	5.6598 (2), 27.1299 (5), 6.9417 (2)	4.7195 (2), 16.9565 (6), 12.6172 (4)	3.7639 (5), 6.5389 (12), 15.141 (3)
α, β, γ (°)	90, 110.693 (2), 90	90, 110.830 (2), 90	90, 100.6230 (10), 90	80.829 (6), 83.770 (5), 86.189 (5)
V (Å^3)	979.20 (5)	996.23 (5)	992.40 (6)	365.24 (11)
Z	4	4	4	2
μ (mm^{-1})	0.08	0.08	0.10	0.11
Crystal size (mm)	0.40 × 0.30 × 0.06	0.30 × 0.20 × 0.08	0.26 × 0.12 × 0.06	0.40 × 0.19 × 0.04
Data collection				
Diffractometer	Bruker SMART CCD area detector system	Bruker SMART CCD area detector system	Bruker SMART CCD area detector system	Rigaku R-AXIS RAPID IP detector system
Absorption correction	Empirical (using intensity measurements) using *SADABS*	Empirical (using intensity measurements) using *SADABS*	Empirical (using intensity measurements) using *SADABS*	Empirical (using intensity measurements) using *ABSCOR*
T_{min}, T_{max}	0.968, 0.995	0.976, 0.994	0.975, 0.994	0.956, 0.996
No. of measured, independent and observed [$I > 2\sigma(I)$] reflections	15 452, 2851, 2498	15 755, 2890, 2048	15 707, 2888, 2061	2550, 1310, 1120
R_{int}	0.028	0.060	0.072	0.022
Refinement				
$R[F^2 > 2\sigma(F^2)]$, $wR(F^2)$, S	0.036, 0.105, 1.11	0.049, 0.130, 1.03	0.040, 0.103, 0.97	0.042, 0.161, 1.10
No. of reflections	2851	2890	2888	1310
No. of parameters	172	242	181	126
No. of restraints	0	158	0	0
H-atom treatment	Only H-atom coordinates refined	H atoms treated by a mixture of independent and constrained refinement	Only H-atom coordinates refined	Only H-atom coordinates refined
$\Delta\rho_{max}, \Delta\rho_{min}$ (e Å^{-3})	0.36, −0.20	0.23, −0.21	0.37, −0.22	0.18, −0.28

	(5)	(6)	(7)	(8)
Crystal data				
Chemical formula	$C_8H_8N_4O$	$C_6H_2Cl_3N_3$	$C_6H_3Br_2N_3$	$C_6H_2Br_3N_3$
M_r	176.18	222.46	276.93	355.84
Crystal system, space group	Orthorhombic, *Pbca*	Monoclinic, $P2_1$	Monoclinic, $P2_1/c$	Monoclinic, $P2_1/n$
Temperature (K)	80	80	80	80
a, b, c (Å)	7.1342 (2), 19.2898 (5), 25.4147 (6)	3.7715 (1), 13.1451 (2), 8.3333 (2)	15.4939 (1), 29.0284 (2), 7.3042 (1)	3.8918 (1), 14.6900 (3), 15.6965 (4)
β (°)	90	102.138 (1)	100.0241 (3)	95.665 (1)
V (Å^3)	3497.50 (16)	403.90 (2)	3235.01 (5)	892.99 (4)
Z	16	2	16	4
μ (mm^{-1})	0.10	1.07	9.96	13.50
Crystal size	0.30 × 0.30 × 0.20	0.40 × 0.15 × 0.10	0.30 × 0.30 × 0.20	0.30 × 0.15 × 0.15
Data collection				
Diffractometer	Bruker SMART CCD area detector system	Bruker SMART CCD area detector system	Bruker SMART CCD area detector system	Bruker SMART CCD area detector system
Absorption correction	Empirical (using intensity measurements) using *SADABS*	Empirical (using intensity measurements) using *SADABS*	Empirical (using intensity measurements) using *SADABS*	Empirical (using intensity measurements) using *SADABS*
T_{min}, T_{max}	0.972, 0.981	0.674, 0.900	0.154, 0.241	0.107, 0.237
No. of measured, independent and observed [$I > 2\sigma(I)$] reflections	52 542, 5073, 4051	6446, 2367, 2291	51 587, 9434, 7032	14 037, 2611, 2312
R_{int}	0.049	0.030	0.069	0.041
Refinement				
$R[F^2 > 2\sigma(F^2)]$, $wR(F^2)$, S	0.040, 0.112, 1.03	0.023, 0.055, 1.05	0.041, 0.084, 1.06	0.022, 0.054, 1.02
No. of reflections	5073	2367	9434	2611
No. of parameters	299	117	433	115
No. of restraints	0	1	0	0

Table 1 (continued)

	(5)	(6)	(7)	(8)
H-atom treatment	Only H-atom coordinates refined	Only H-atom coordinates refined	Only H-atom coordinates refined	Only H-atom coordinates refined
$\Delta\rho_{max}$, $\Delta\rho_{min}$ (e Å^{-3})	0.29, −0.23	0.34, −0.47	0.81, −0.90	0.79, −1.35

Computer programs used: *SMART* (Siemens, 1995), *SAINT* (Bruker, 2007), *SADABS* (Bruker, 2004*a*), *TEXSAN* (Molecular Structure Corporation, 1999), *ABSCOR* (Higashi, 1995), *SHELXS*97, *SHELXL*97 (Sheldrick, 2008), *ORTEP*3 for Windows (Farrugia, 1997).

2.3.2. Crystal structure analysis. Each structure was solved by direct methods using the *SHELXS*97 program (Sheldrick, 2008) and was refined by full-matrix least-squares using the *SHELXL*97 program (Sheldrick, 2008). All non-H atoms were refined anisotropically. All H atoms were located in the difference Fourier map and were refined isotropically.

2.3.3. Photo-irradiation. A single crystal, which was rotated slowly on the diffractometer, was cooled with the cold-nitrogen gas-flow method to 80 K and was photo-irradiated using the light-guide tube from a high-pressure Hg lamp (SAN-EI UVF-352S, 350 W), the top of the tube being 7 cm from the crystal. Light with wavelengths longer than 420 nm was irradiated by inserting a filter (L42 TOSHIBA) between the top of the tube and the crystal. The diffractometer was covered with a black sheet to avoid room light during data collection and photo-irradiation. The crystals changed their colors from transparent or pale yellow to red–brown or yellow from 1.5 to 3.0 h after the beginning of the photo-irradiation.

2.3.4. Crystal-structure analysis after photo-irradiation. Only crystal (2) kept the single-crystal form after photo-irradiation for 5 h. The other crystals were easily broken or unchanged within 3 h of photo-irradiation. However, the unchanged crystals decomposed after prolonged photo-irradiation. The X-ray diffraction data of (2) after photo-irradiation were collected under the same conditions as before irradiation. The crystal data and experimental details of (2) after photo-irradiation (2′) are also listed in Table 1. The cell volume increased and the crystal color changed from colorless to pale brown. The volume change suggested that the total structure of the photoproduct is larger than that of the reactant azide molecule. At the initial stage of the refinement, the structure of the reactant molecule including H atoms, which was assumed to be the same as that before photo-irradiation, was treated as a rigid group and only the rotation and translation of the rigid group were introduced. The photoproducts appeared on the difference map with low occupancy, although they were heavily overlapped with the reactant azide molecule. Refinement of the original azide molecule and the new photoproducts were performed alternatively, such that one was refined with a rigid-body model if the other was refined with restraints. The H atoms of the arylnitrene produced were not included at this stage. The bond distances, bond angles and anisotropic displacement parameters of the azide molecule and arylnitrene were restrained to have the same values as the corresponding ones of the original molecule. The N—N distance of dinitrogen was restrained to 1.098 Å (Kagakubinran Kisohen II, 2001). At the final stage, the parameters of arylnitrene and dinitrogen were refined with restraints and those of the azide molecule were refined with the rigid-body model. The occupancy factors of the photo-produced dinitrogen molecule and the original azido group were also refined as x and $1 - x$. The x parameter converged to 0.199 (5). The H atoms of arylnitrene were obtained geometrically (C—H = 0.95 Å) and were included in the least-squares with the riding-atom model. The maximum peak and hole in the final difference electron-density map were +0.23 (0.65 Å from N13*B*) and −0.21 e Å^{-3} (0.77 Å from N11).

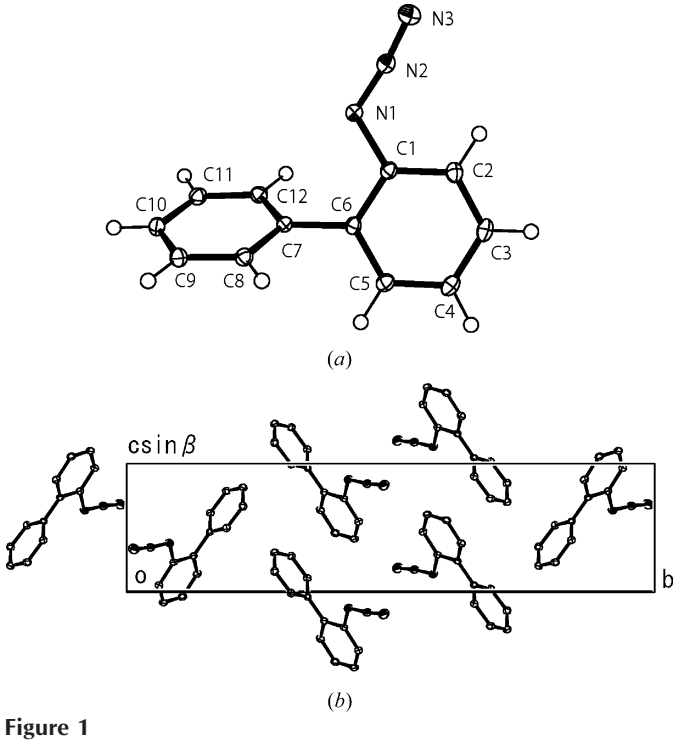

Figure 1
(*a*) Molecular structure and (*b*) crystal structure viewed along the *a* axis of (2) before photo-irradiation. The displacement ellipsoids of the atoms are drawn at the 50% probability level. The circles of the H atoms are drawn on an arbitrary scale.

3. Results

3.1. Structures of (2) before and after photo-irradiation

The molecular and crystal structures of (2) before photo-irradiation are shown in Figs. 1(*a*) and (*b*). The azide molecule has fairly loose contacts with the surrounding molecules. Two azido groups are aligned across an inversion center. The azido group is almost coplanar with the attached benzene ring, the torsion angle of N2—N1—C1—C2 being −4.9 (1)°. The two

benzene rings of the biphenyl group are not coplanar and have an angle of 61.2 (1)° between them. This is because of the short contact between N1 and C12, 3.091 (1) Å. The contact between N1 and H12, 2.91 (1) Å, is not short, probably owing to the large torsion angle of the biphenyl group.

The difference electron-density map before photo-irradiation is shown in Fig. 2(*a*). The residual electron density can be interpreted as bonding electrons. After photo-irradiation, the difference electron-density map is shown in Fig. 2(*b*), in which the calculated electron density using the structure before photo-irradiation was subtracted from the observed one. A new residual peak, +0.84 e Å^{-3} (0.40 Å from N3), and a hole, −0.47 e Å^{-3} (0.58 Å from N2), appear in the vicinity of the azido group. The difference map indicates that the 2-azidobiphenyl molecule is transformed to dinitrogen and 2-biphenylnitrene molecules. The refined structure is shown in Fig. 3.

Although it is clear that 2-biphenylnitrene was observed, it is difficult to discuss its precise structure since strong restraints were applied to separate the photoproducts from the over-

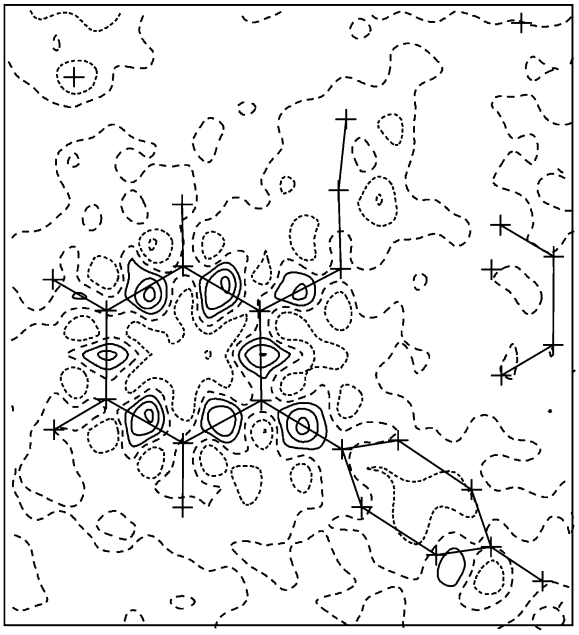

(*a*)

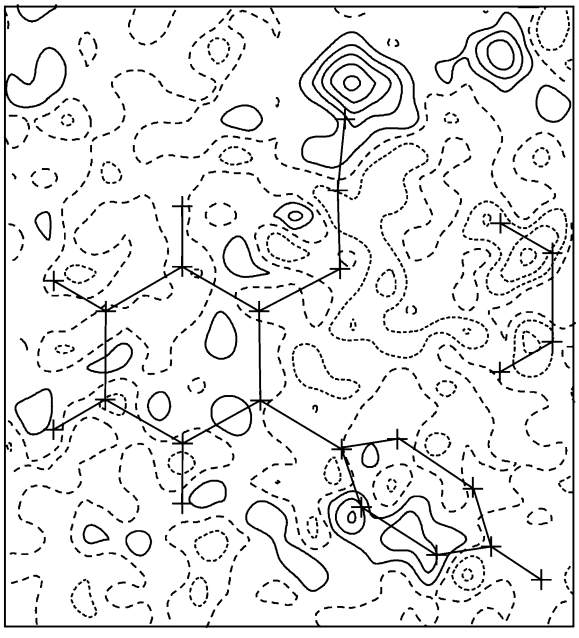

(*b*)

Figure 2
(*a*) Difference electron-density map of (2) before photo-irradiation and (*b*) difference electron-density map of (2) after photo-irradiation minus the corresponding map before photo-irradiation. The contour interval for both drawings is 0.1 e Å^{-3}. The solid and dotted lines indicate the positive and negative peaks.

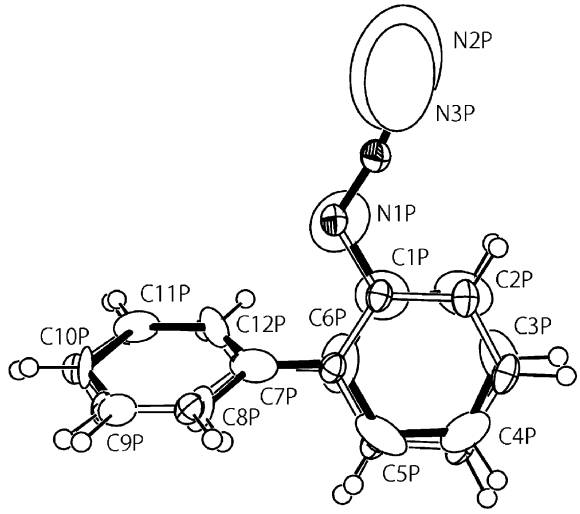

Figure 3
Molecular structure after photo-irradiation. The displacement ellipsoids are at the 50% probability level. Molecules with black bonds and open bonds indicate the structures before and after photo-irradiation.

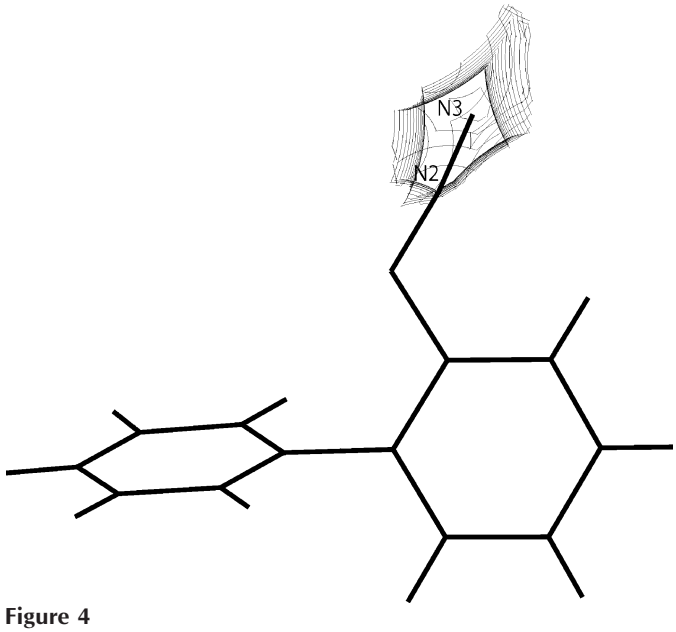

Figure 4
The reaction cavity for the N2 and N3 moiety.

lapped azide molecule. However, the by-product, the dinitrogen molecule, shows its unique behavior in the crystal lattice. Fig. 4 shows the reaction cavity around the N2 and N3 moiety. The dinitrogen molecule is captured in the cavity. The large temperature factors indicate an orientational disorder in the cavity.

3.2. Structures of the other crystals before photo-irradiation

The molecular and crystal structures of (3) are shown in Figs. 5(*a*) and (*b*). Two hydrogen bonds between the carboxyl groups of two molecules around an inversion center form a dimer structure. The O—H and O···O distances and the O1—H1···O2 hydrogen-bond angle are 0.91 (2) and 2.686 (1) Å, and 178 (2)°, respectively. The dimers stack along the *a* axis. The azido group is almost coplanar with the benzene ring, the torsion angle of N2—N1—C1—C6 being −5.1 (2)°. The alkyl chain from C7 to C9, including the C4 and C10 atoms, takes the *trans* conformation and is approximately planar. The average alkyl plane makes angles of 84.4 (1) and 20.5 (7)° with the benzene and carboxyl planes.

The molecular and crystal structures of (4) are shown in Figs. 6(*a*) and (*b*). Two hydrogen bonds between the carboxyl groups of the two molecules around an inversion center form a dimer structure. The O—H and O···O distances and the O1—H1···O2 hydrogen bond angle are 1.10 (5) and 2.617 (2) Å, and 176 (4)°, respectively. The two azido groups also contact each other around another inversion center, the contact between the azido groups (N1···N1′) being 3.093 (3) Å. The molecules are stacked as a column along the *a* axis. The

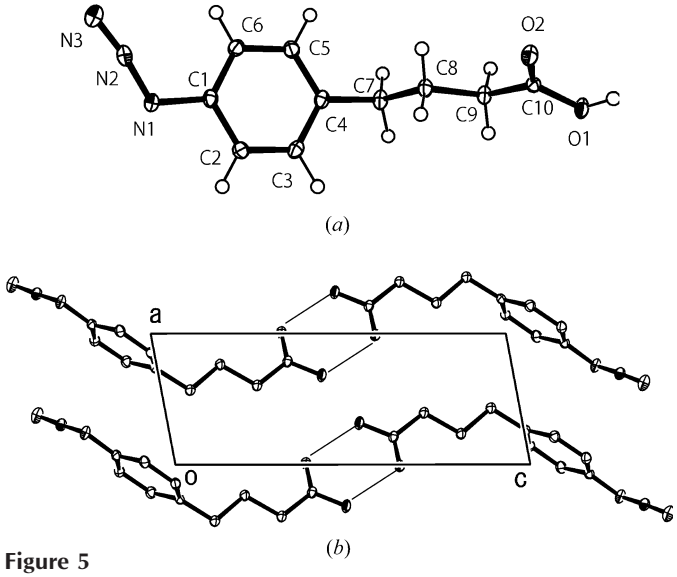

Figure 5
(*a*) Molecular structure of (3) and (*b*) the crystal structure viewed along the *b* axis before photo-irradiation. The displacement ellipsoids are drawn at the 50% probability level. The circles of the H atoms are drawn on an arbitrary scale. The broken lines indicate hydrogen bonds.

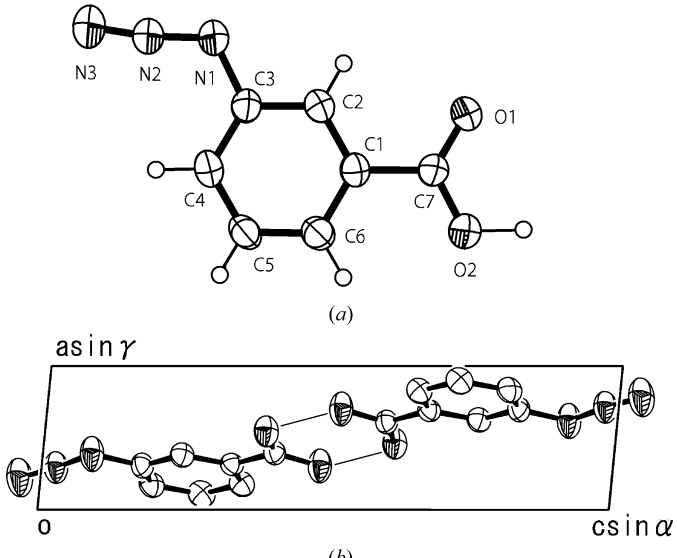

Figure 6
(*a*) Molecular structure of (4) and (*b*) the crystal structure viewed along the *b* axis before photo-irradiation. The displacement ellipsoids are drawn at the 50% probability level. The circles of the H atoms are drawn on an arbitrary scale. The broken lines indicate hydrogen bonds.

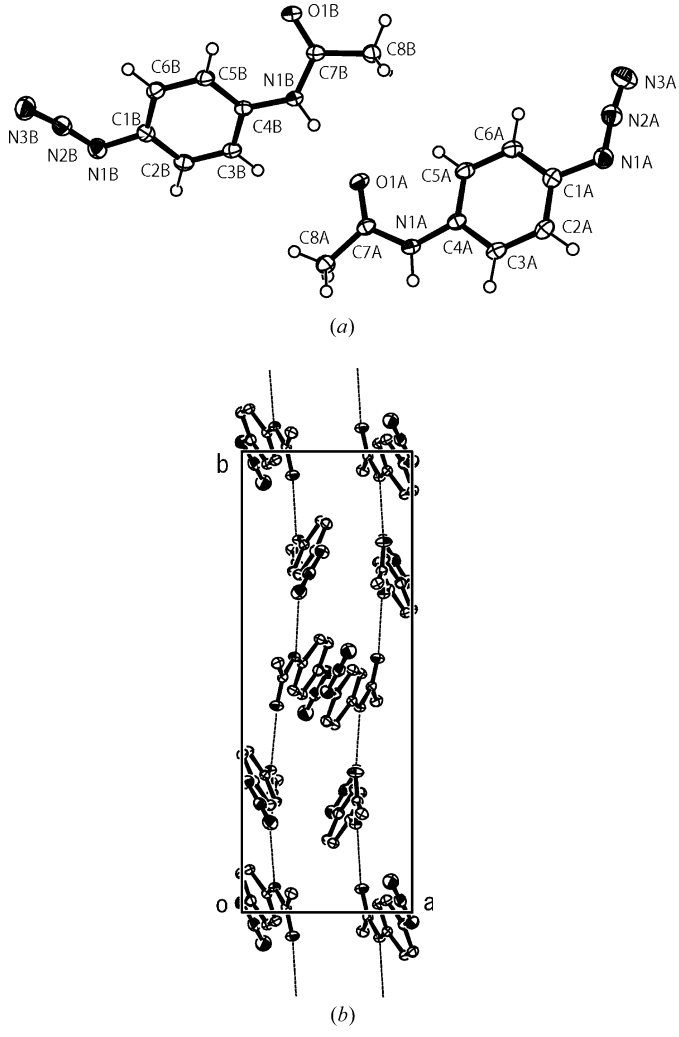

Figure 7
(*a*) Molecular structure of (5) and (*b*) the crystal structure viewed along the *o* axis before photo-irradiation. The displacement ellipsoids are drawn at the 50% probability level. The circles of the H atoms are drawn on an arbitrary scale. The broken lines indicate hydrogen bonds.

Table 2
Crystal density and volume of the reaction cavity in each crystal.

Crystal	1	2	3	4	5	6	7	8
Density (g cm^{-3})	1.555	1.324	1.374	1.528	1.338	1.829	2.274	2.647
Cavity (Å^3)	2.35	2.64	1.38	1.64	2.28 2.75	1.19	1.80 1.68 1.94 1.96	1.41

carboxyl and azido groups are approximately coplanar with the central benzene ring. The dihedral angle between the carboxyl and phenyl groups is 8.3 (4)° and the torsion angle of N2—N1—C3—C4 is 8.3 (4)°.

The molecular and crystal structures of (5) are shown in Figs. 7(*a*) and (*b*). There are two crystallographically independent molecules, *A* and *B*, in an asymmetric unit. The intermolecular N—H···O hydrogen bonds connect the *A* and *B* molecules alternately as a chain along the *b* axis. The N—H and N···O distances and the angle of N—H···O of the two hydrogen bonds are 0.90 (2) and 2.871 (1) Å and 173 (1)°, for N4*A*—H4*A*···O1*B*, and 0.89 (2) and 2.853 (1) Å and 173 (1)°, for N4*B*—H4*B*···O1*A*. The hydrogen-bonding chains are stacked along the *a* axis. The torsion angles of the *A* and *B* azido groups of N2*A*—N1*A*—C1*A*—C6*A* and N2*B*—N1*B*—C1*B*—C6*B* are −10.4 (2) and −8.6 (2)°. The amido groups make angles of 11.77 (6) and 30.65 (6)° with the central benzene ring for molecules *A* and *B*.

The molecular and crystal structures of (6), (7) and (8) are given in the supplementary material. There are no unusual short contacts between the molecules in these crystal structures.

4. Discussion

4.1. Photo-reaction of (2)

2-Azidobiphenyl and its derivatives have been studied intensively since it was reported that 2-azidobiphenyl gave carbazole by heat or UV light, as shown in Scheme (IV) (Smith & Brown, 1951). Then the direct irradiation of 2-azidobiphenyl in various solutions was reported to produce carbazole and azo-2-biphenyl with yields of 68–74% and 8–12% (Swenton *et al.*, 1970). The UV photolysis of 2-azidobiphenyl in the solid state showed that the product ratio of azo-2-biphenyl to carbazole was 1.0 at 123 K, but that the ratio decreased to 0.22 at 253 K (Sasaki *et al.*, 1998). The ultrafast laser flash photolysis revealed that the singlet 2-biphenylnitrene was produced in glassy 3-methylpentane at 77 K and that gradually changed to the triplet one with lower energy than that of the singlet one. In the fluid solution the singlet 2-biphenylnitrene was transferred to carbazole through isocarbazole. The intersystem crossing converted the singlet 2-biphenylnitrene to the triplet one, which was dimerized to azo-2-biphenyl (Tsao *et al.*, 2003).

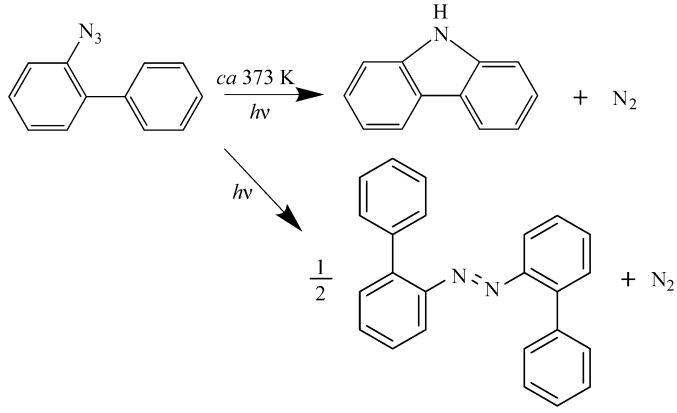

(IV)

It is clear why the carbazole or azobenzene is not produced in the photoreaction of (2) at 80 K. The intramolecular distance between N1 and C12 is 3.092 (1) Å. The dihedral angle between the two phenyl groups is large, 61.2 (1)°, to avoid steric repulsion with the azido group. The lifetime of the singlet 2-biphenylnitrene was reported to be 59 ns at 77 K (Tsao *et al.*, 2003). In order to produce carbazole, the N1 and C12 atoms must approach each other within a nanosecond by a rotation around the C6—C7 bond. However, the rotation of the phenyl rings may be strongly suppressed in the crystal structure at 80 K. Therefore, the singlet 2-biphenylnitrene easily transferred to the triplet.

On the other hand, the closest contact of (2) is related by an inversion center and the distance between the N1 atoms is 4.644 (2) Å. As the distance is too large, it may be difficult to consider that the photo-produced 2-biphenylnitrene molecules around an inversion center come close to each other and make a dimer during photo-irradiation at 80 K. For these reasons, only the triplet 2-biphenylnitrene can be observed in the crystal after photo-irradiation.

UV photolysis of 2-azidobiphenyl in the solid state showed that the product ratio of azo-2-biphenyl to carbazole was 1.0 at 123 K, but that the ratio decreased to 0.22 at 253 K (Sasaki *et al.*, 1998). This suggests that the conformational change of 2-biphenylnitrene (a rotation around the C6—C7 bond) may be easier than the migration to form the dimer in the crystalline lattice at higher temperatures.

4.2. Reaction cavity

When single crystals of (1)–(8) were irradiated with UV light, (1) and (2) were partially changed to benzofuroxan and 2-biphenylnitrene, whereas the other crystals showed no change or were broken. Table 2 shows the volume of the reaction cavity for the N2 and N3 atoms of the azido group and the density in each crystal before photo-irradiation. Since each crystal showed a color change and the ESR signal of the triplet nitrene was observed after photo-irradiation, the photo-reaction proceeded on the surface of the crystal. If the inner molecules undergo the photoreaction with retention of the single-crystal form, it seems necessary to have enough void space around the azido group to accommodate the dinitrogen

molecule produced. Since crystals of (1) and (2) have large cavity volumes, the reaction proceeded partially in the crystal. Crystal (5) also has a large cavity volume. However, the crystal was easily broken when it was photo-irradiated. As shown in Fig. 7(*b*), the crystal structure has sheets composed of the azido group, perpendicular to the *c* axis (z = 0.25 and 0.75). If the photoreaction occurs, the dinitrogen molecules produced may go out of the crystal along the walls. For this reason the crystal was easily broken during photo-irradiation. Since the cavity volumes of the other crystals are less than 2.0 Å^3, the reaction occurred only at the surface of the crystal. It must be emphasized that although the crystal of (3) has smaller density than that of (1), the reaction was not observed owing to the smaller size of the reaction cavity than that of (1).

The authors thank Drs S. Taniguchi and G. Harada for their help in the ESR measurement. This work was supported by a Grant-in-Aid from MEXT.

References

Bertho, A. (1924). *Chem. Ber.* **57**, 1138–1142.

Borden, W. T., Gritsan, N. P., Hadad, C. M., Karney, W. L., Kemnitz, C. R. & Platz, M. S. (2000). *Acc. Chem. Res.* **33**, 765–771.

Bruker (2004*a*). *SADABS*. Bruker AXS Inc., Madison, Wisconsin, USA.

Bruker (2004*b*). *XPREP*. Bruker AXS Inc., Madison, Wisconsin, USA.

Bruker (2007). *SAINT*. Bruker AXS Inc., Madison, Wisconsin, USA.

Farrugia, L. J. (1997). *J. Appl. Cryst.* **30**, 565.

Gritsan, N. P. & Plats, M. S. (2001). *Adv. Phys. Org. Chem.* **36**, 255–304.

Higashi, T. (1995). *ABSCOR*. Rigaku Corporation, Tokyo, Japan.

Iddon, B., Meth-Cohn, O., Scriven, E. F. V., Suschitzky, H. & Gallagher, P. T. (1979). *Angew. Chem. Int. Ed.* **18**, 900–917.

Kagakubinran Kisohen II. (2001). *The Chemical Society of Japan*, p. 652. Maruzen, Japan.

Karney, W. L. & Borden, W. T. (2001). *Adv. Carbene Chem.* **3**, 205–247.

Kawano, M., Takayama, T., Uekusa, H., Ohashi, Y., Ozawa, Y., Matsubayashi, K., Imabayashi, H., Mitsimi, M. & Toriumi, K. (2003). *Chem. Lett.* pp. 922–923.

Kotzyba-Hibert, F., Kapfer, I. & Goeldner, M. (1995). *Angew. Chem. Int. Ed.* **34**, 1296–1312.

Mahé, L., Izuoka, A. & Sugawara, T. (1992). *J. Am. Chem. Soc.* **114**, 7904–7906.

Meijer, E. W., Nijhuis, S. & Vroonhoven, F. C. B. M. V. (1988). *J. Am. Chem. Soc.* **110**, 7209–7210.

Mitsumori, T., Sekine, A., Uekusa, H. & Ohashi, Y. (2010). *Acta Cryst.* B**66**, 647–661.

Molecular Structure Corporation (1999). *TEXSAN for Windows*. Version 1.06. Molecular Structure Corporation, The Woodlands, Texas, USA.

Platz, M. S. (1995). *Acc. Chem. Res.* **28**, 487–492.

Reiser, A., Bowers, G. & Horne, R. J. (1966). *Trans. Faraday Soc.* **62**, 3162–3169.

Reiser, A. & Frazer, V. (1965). *Nature*, **208**, 682–683.

Sasaki, A., Mahé, L., Izuoka, A. & Sugawara, T. (1998). *Bull. Chem. Soc. Jpn*, **71**, 1259–1275.

Scriven, E. F. V. (1984). *Azides and Nitrenes Reactivity and Utility*. New York: Academic Press.

Sheldrick, G. M. (2008). *Acta Cryst.* A**64**, 112–122.

Siemens (1995). *SMART*. Siemens Analytical X-ray Instruments Inc., Madison, Wisconsin, USA.

Smolinski, G., Wasserman, E. & Yager, W. A. (1962). *J. Am. Chem. Soc.* **84**, 3220–3221.

Smith, P. A. S. & Brown, B. B. (1951). *J. Am. Chem. Soc.* **73**, 2435–2437.

Swenton, J. S., Ikeler, T. J. & Williams, B. H. (1970). *J. Am. Chem. Soc.* **92**, 3103–3109.

Takayama, T., Kawano, M., Uekusa, H., Ohashi, Y. & Sugawara, T. (2003). *Helv. Chim. Acta*, **86**, 1352–1358.

Tsao, M.-L, Gritsan, N., James, T. R., Platz, M. S., Hrovat, D. A. & Borden, W. T. (2003). *J. Am. Chem. Soc.* **125**, 9343–9358.

Wentrup, C. (1981). *Adv. Heterocycl. Chem.* **28**, 231–361.